JOURNAL OF MATERIALS SCIENCE 17 (1982) 547–557

Micromechanics approach to the indentation hardness of glass matrix particulate composites

N. MIYATA, H. JINNO
Department of Industrial Chemistry, Faculty of Engineering, Kyoto University, Sakyo-ku, Kyoto 606, Japan

A theoretical analysis is made of the indentation hardness of glass matrix, particulate composites. It is hypothesized that glass is an elastic–plastic solid on a microscopic scale. Based upon the Marsh theory of indentation, expressions are formulated for indentation hardness of two-phase composites containing spherical particles. When hard particles are dispersed in a soft glass matrix, the overall hardness depends upon the matrix hardness, the volume-fraction of dispersed phase, the elastic properties of the two phases and also the matrix flow stress. On the other hand, when soft particles are dispersed in a hard glass matrix, the hardness and the elastic moduli vary in parallel with the volume-fraction of dispersed phase. Furthermore, the present analysis indicates that the hardness of a composite is independent of the particle size and interparticle spacing if the volume-fraction of the particles is kept constant. Experimental results of the Vickers hardness of phase-separated glasses as well as published hardness data for a glass-ceramic are used for the verification of the theory. The proposed theory explains well the hardness behaviour of such glass matrix composites in terms of the properties and amounts of the individual phases and the microstructural effects.

1. Introduction

Many investigations have been undertaken to correlate the indentation hardness of glass with its other physical properties and to interpret indentation behaviour in terms of glass structure. Although the mechanism of deformation during indentation is not clearly understood, hardness testing provides useful information concerning the mechanical behaviour of glass.

It is well-known that the mechanical properties, including hardness, are sensitive to inhomogeneities in the microstructure of materials. As for inhomogeneous glasses or glass-ceramics, however, little detailed work has been done concerning the relationship of indentation hardness to their microstructure. Donald and McCurrie [1] measured the indentation hardness of an $MgO–Li_2O–Al_2O_3–SiO_2$ glass-ceramic as a function of heat-treatment time, determining the microstructure by replication electron microscopy. They showed that the hardness correlates to some extent with the changes in microstructure. Stryjak and McMillan [2, 3] studied the variation of hardness with heat-treatment of a spinel transparent glass-ceramic based on the $ZnO–Al_2O_3–SiO_2$ system. They found that the hardness increased linearly with the volume-fraction and particle size of the crystallites developed. Rice [4] discussed their experimental results and interpreted them, taking into account a possible internal stress dependence of the hardness of crystallized glasses. Turetzky, Jenkins and Fraser [5] studied the Vickers hardness of sintered films of borosilicate glass on alumina substrates. They observed a wide dispersion of hardness of the heat-treated samples, and qualitatively attributed this phenomenon to the extent of phase-separation in the samples, although no interpretation in relation to the phase-separated morphology was given.

The present paper is concerned with the effect

0022–2461/82/020547–11$3.10/0

of second-phase dispersion on the indentation behaviour of glass matrix, particulate composites. A theory is proposed for a model two-phase particulate system where the particle size is much smaller than the scale of deformation produced by indentation. Expressions are formulated for the indentation hardness of such solids, based upon a micromechanical viewpoint of flow in glass. For the verification of the theory, the Vickers indentation hardness measurements are carried out on phase-separated lead borate and sodium borosilicate glasses. The theoretical results are also compared with published hardness data for a glass-ceramic having particulate microstructure.

2. A brief review of the theories of indentation hardness of glass

2.1. Mechanism of deformation in glass

The mechanism of deformation during indentation, which results in a permanent impression in glass, has long been a subject of controversy. Some mechanisms have been suggested by several authors: They are (a) viscous flow [6], (b) plastic flow [7–9] and (c) densification resulting from compression and shear [10, 11]. The experimental results of the Vickers hardness of soft glasses may best be interpreted by introducing the concept of "plastic flow" which is somewhat analogous to that which occurs in metals. However, in the case of hard glasses such as pure silica, there is some evidence for the occurrence of densification phenomena. At the present stage of development of the deformation theory of glass, it is difficult to specify in a quantitative manner which of these two basic processes dominates in a given glass. Peter [12] discussed some phenomena which may be observed during indentation in silicate glasses and suggested that the flow in glass at room temperature appears to require a minimum percentage of network modifiers. It seems reasonable to assume that indentation involves both shear-induced flow (either plastic or viscous) and pressure-induced densification, the proportions of which depend upon the nature of glass, although atomistic displacement mechanisms are still unknown.

2.2. The Marsh theory

The Vickers hardness test method is one of the most common and reliable methods for indentation hardness measurements. The Vickers hardness is defined as the load divided by the pyramidal area of indentation, i.e., the mean pressure under the indenter. It is well known that, for softer materials, the Vickers hardness, H, can be closely related to the yield stress, σ_y, as considered by Tabor [13] $H/\sigma_y \simeq 3$. However, this simple indentation theory does not hold for highly elastic materials which show large elastic strains before the onset of plastic flow.

For highly elastic materials, an adequate simple model for the elastic–plastic indentation problem is that of the expansion of a spherical cavity in an elastic–plastic medium by internal pressure. Hill [14] derived an expression for this pressure, p, required to expand a spherical cavity in an infinite medium

$$\frac{p}{\sigma_y} = \frac{2}{3} + \left(\frac{2}{3}\right) \ln\left(\frac{E}{3(1-\nu)\sigma_y}\right), \qquad (1)$$

where σ_y is the yield stress in compression, E is the Young's modulus and ν is the Poisson's ratio. Marsh [9] proposed a hardness theory based upon the Hill equation and derived a similar expression for the indentation

$$\frac{H}{\sigma_y} = A + B\left(\frac{3}{3-\xi}\right) \ln\left(\frac{3}{\xi + 3\delta - \xi\delta}\right), \qquad (2)$$

where $\xi = 6(1-2\nu)\sigma_y/E$, $\delta = (1+\nu)\sigma_y/E$, and A and B are constants. Generally $\sigma_y/E \ll 1$, hence $\xi \ll 1$ and $\delta \ll 1$. Although Marsh used a more precise Hill equation, eliminating certain simplifying assumptions, Equation 2 may be approximated with acceptable accuracy by the form

$$\frac{H}{\sigma_y} = A + B \ln\left(\frac{E}{3(1-\nu)\sigma_y}\right). \qquad (3)$$

Marsh carried out some experiments on a wide range of materials with varying σ_y/E, and found empirically that $A = 0.28$ and $B = 0.60$ for a hemi-spherical cavity. Assuming that Equation 2 is applicable to glasses, he calculated values of flow stresses for various glasses by indentation hardness measurements.

3. Indentation hardness of glass matrix, particulate composites

As discussed briefly in Section 2.1, recent studies indicate that the indentation of glass involves both plastic flow and densification mechanisms. Preferably, the analysis of the hardness of glass matrix composites should be undertaken, based upon a pertinent model which takes into account the contributions of these two possible deformation mech-

anisms. However, such a model is difficult to establish at the present stage of studies on the deformation of glass. In the absence of detailed knowledge of densification phenomena during the indentation of glass, the authors make the hypothesis that glass is an elastic–plastic solid on a microscopic scale. For many glasses where the contribution of densification process to the overall deformation process is presumed to be small, this hypothesis may be quite reasonable: it can explain, at least at a phenomenological level, a great variety of observations of deformation phenomena in glasses. Furthermore, high fracture surface energy values observed for many glasses [15] suggest that glass may exhibit a limited plastic deformation under the very high stresses.

In the following sections, we will analyse (regarding glasses as elastic–plastic materials) the indentation hardness of glass matrix, particulate composites. As shown in the preceding section, the indentation hardness of elastic–plastic materials is related to their yield stresses. The problem of analysing the hardness of a composite, therefore, resolves into that of finding its yield stress. For this purpose, micromechanics of composites will be applied to the considered composite system.

3.1. Analytical model

The model used for the present considerations is a two-phase composite consisting of spherical crystalline or glass particles embedded in a glass matrix. It is assumed that the mechanical properties of each phase are homogeneous and perfectly isotropic. It is further assumed that the dispersed particle size is much smaller than the scale of deformation produced by indentation.

After recalling the effective elastic moduli of a body containing dispersed spherical inclusions, the hardness of particulate composites will be considered successively for two cases, where (a) the elastic limit of the particles is higher than that of the matrix and conversely (b) the elastic limit of the particles is lower than that of the matrix.

3.2. Effective elastic moduli of a composite containing spherical particles

Elastic properties are one of the important factors which determine the deformation behaviour of composite materials. Here the knowledge of the effective elastic moduli of a composite containing second-phase particles is recalled.

For a dispersion of spherical particles in a continuous matrix, Kerner [16] and Hashin [17] have given the expressions for the bulk modulus, K, and the shear modulus, μ, of the composite as follows

$$K = K_m + \phi\left[\frac{1}{K_p - K_m} + \frac{3(1-\phi)}{3K_m + 4\mu_m}\right]^{-1}, \quad (4)$$

and

$$\mu = \mu_m + \phi\left[\frac{1}{\mu_p - \mu_m} + \frac{6(K_m + 2\mu_m)(1-\phi)}{5\mu_m(3K_m + 4\mu_m)}\right]^{-1}, \quad (5)$$

where the subscripts m and p refer to the matrix and particle, respectively, and ϕ is the volume-fraction of dispersed particles. The Young's modulus of the composite can be calculated according to the following equation

$$E = \frac{9K\mu}{3K + \mu}. \quad (6)$$

For a dilute dispersion of spherical particles, μ can be expressed as [17, 18]

$$\mu = \frac{\mu_m}{1 - \left(\frac{\mu_p - \mu_m}{\mu_p}\right) Q\phi} = \frac{\mu_m}{1 - \alpha\phi}, \quad (7)$$

with

$$Q = \frac{15(1-\nu_m)\mu_p}{(7-5\nu_m)\mu_m + (8-10\nu_m)\mu_p}, \quad (8)$$

and

$$\alpha = \left(1 - \frac{\mu_m}{\mu_p}\right)Q = \frac{15(1-\nu_m)}{7-5\nu_m}(Q-1), \quad (9)$$

where ν_m is the Poisson's ratio of the matrix. Since $0.15 \lesssim \nu \lesssim 0.35$ for most materials, then $1 \leqslant Q \lesssim 2$ and $0 \leqslant \alpha \lesssim 2$ for $\mu_p \geqslant \mu_m$ and $0 \lesssim Q < 1$ and $-2 \lesssim \alpha < 0$ for $\mu_p < \mu_m$.

The bulk modulus, K, and the Young's modulus, E, can be also expressed, for a dilute concentration of spherical particles, in the same form as Equation 7

$$K = \frac{K_m}{1 - \left(\frac{K_p - K_m}{K_p}\right) Q'\phi} = \frac{K_m}{1 - \alpha'\phi} \quad (10)$$

and

$$E = \frac{E_m}{1 - \left(\frac{E_p - E_m}{E_i}\right) Q''\phi} = \frac{E_m}{1 - \alpha''\phi}. \quad (11)$$

Note that Q corresponds to the shear stress concentration factor in the inclusion [18]. Similarly, Q' and Q'' are the bulk and normal stress concentration factors in the inclusion. It should be also noted that, if the Poisson's ratios of the matrix and inclusion are nearly equal and take values near 0.25, $\mu/\mu_m \simeq K/K_m \simeq E/E_m$ according to Equations 4 to 6.

3.3. Dispersion of second-phase particles having high elastic limit

If the dispersed phase has higher yield stress, the plastic flow may be restricted in a glass matrix and the yield stress of the matrix may be more or less modified by the presence of hard particles. It has been shown that the presence of non-deforming particles in a ductile material which can exhibit a large plastic deformation not only affects the overall yield stress but also exerts a large work-hardening effect [19]. However, this is not the case for glass matrix composites where only a limited plastic deformation is assumed to occur in the matrix. It can be then considered that the dispersion of hard particles in the glass matrix contributes to modifying the yield stress but causes little or no work-hardening effect. For the present case, the analysis will be performed for small volume-fractions of dispersed particles at which the interaction between particles can be neglected.

When a glass matrix composite containing hard particles is subjected to a uniform externally applied shear stress, τ, the macroscopic shear strain, γ, is represented, before the onset of plastic flow in the matrix, as

$$\gamma = \tau/\mu. \tag{12}$$

According to Eshelby [18], the state of stress in a tri-axial ellipsoidal inclusion in a matrix is uniform when the state of stress or strain at infinity is uniform. For a dilute concentration of dispersed spherical particles, the shear stress, τ_p, and shear strain, γ_p, of the particle is given by [18]

$$\tau_p = Q\tau \tag{13}$$

and

$$\gamma_p = Q\tau/\mu_p, \tag{14}$$

where Q is the shear stress concentration factor arising as a consequence of the stress interaction between particle and matrix and is given by Equation 8. It is assumed that, as long as the stresses in the matrix do not exceed the elastic limit of the matrix, the macroscopic strain, γ, can be expressed as follows

$$\gamma = (1-\phi)\bar{\gamma}_m + \phi\gamma_p. \tag{15}$$

Here, $\bar{\gamma}_m$ is the average shear strain in the matrix. Taking $\bar{\gamma}_m = \bar{\tau}_m/\mu_m$ where $\bar{\tau}_m$ is the average shear stress in the matrix and using Equation 12 to 14, we obtain from Equation 15

$$\tau\left(\frac{1}{\mu} - \frac{Q}{\mu_p}\phi\right) = (1-\phi)\frac{\bar{\tau}_m}{\mu_m}. \tag{16}$$

On the other hand, for a dilute dispersion of spherical second-phase particles, the effective shear modulus, μ, is given by Equation 7. Then Equation 16 can be written as

$$\tau = \frac{1-\phi}{1-Q\phi}\bar{\tau}_m. \tag{17}$$

For the present case, we assume that the composite body is regarded as being in a state of yielding when the average shear stress in the matrix reaches the yield stress of the matrix. That is, the composite may attain the yielding state when

$$\bar{\tau}_m = \tau_{ym} \qquad \text{i.e., } \bar{\gamma}_m = \gamma_{ym}, \tag{18}$$

where τ_{ym} and γ_{ym} are respectively the yield stress and the yield strain in shear of the matrix without a dispersion. Then the composite yield stress in shear, τ_y, can be expressed from Equation 17, as

$$\tau_y = \frac{1-\phi}{1-Q_\phi}\tau_{ym}. \tag{19}$$

Both the von Mises criterion of yielding and that of Tresca indicate that the yield stress in pure shear is related to the yield stress in uniaxial tension by a proportionality constant [20]. In addition, it can be assumed that the yield stresses in tension and compression are the same. Hence, expressing in terms of the yield stresses in tension or compression, we obtain

$$\sigma_y = \frac{1-\phi}{1-Q\phi}\sigma_{ym}, \tag{20}$$

where σ_y and σ_{ym} are the tensile or compressive yield stresses of the composite and the matrix, respectively.

Now the identation hardness of the present type of particulate composites can be calculated by substituting Equation 20 into Equation 3. It is assumed that the Poisson's ratio of each phase takes equally the same values of about 0.2 to 0.3,

and hence $E/E_m \simeq \mu/\mu_m$. Substitution of Equations 20 and 7 into Equation 3 leads to

$$H = \left(\frac{1-\phi}{1-Q\phi}\right) \times \left(H_m + \sigma_{ym} \cdot B \ln \frac{1-Q\phi}{(1-\alpha\phi)(1-\phi)}\right), \quad (21)$$

where H_m is the hardness of the matrix. Putting

$$\kappa = B\sigma_{ym}/H_m \quad (22)$$

and rearranging Equation 21, we finally obtain

$$\frac{H}{H_m} = \left(1 + \frac{Q-1}{1-Q\phi}\phi\right) \times \left(1 + \kappa \ln \frac{1-Q\phi}{(1-\alpha\phi)(1-\phi)}\right). \quad (23)$$

The quantity, Q, takes values of about 0 to 2, and hence $-2 \lesssim \alpha \lesssim 2$. In the case of very small concentrations of dispersed particles, the logarithmic term in Equation 23 can be approximated as

$$\ln \frac{1-Q\phi}{(1-\alpha\phi)(1-\phi)} \simeq \ln [1 + (\alpha - Q + 1)\phi] \quad (24)$$

$$= \ln \left(1 + \frac{8-10\nu_m}{7-5\nu_m}(Q-1)\phi\right). \quad (25)$$

Since $-1 \lesssim (Q-1) \lesssim 1$, the logarithmic term can be further approximated as follows

$$\ln \left(1 + \frac{8-10\nu_m}{7-5\nu_m}(Q-1)\phi\right) \simeq \frac{8-10\nu_m}{7-5\nu_m}(Q-1)\phi. \quad (26)$$

Then, for such a small ϕ, the indentation hardness can be expressed as

$$\frac{H}{H_m} \simeq \left(1 + \frac{Q-1}{1-Q\phi}\phi\right) \times \left(1 + \kappa \frac{8-10\nu_m}{7-5\nu_m}(Q-1)\phi\right) \quad (27)$$

$$\simeq [1 + (Q-1)\phi][1 + \kappa(Q-1)\phi] \quad (28)$$

$$\simeq 1 + (Q-1)(1+\kappa)\phi. \quad (29)$$

3.4. Dispersion of second-phase particles having low elastic limit

For the case where a matrix with high elastic limit contains second-phase particles with low elastic limit, it can be assumed that the dispersed particles do not act as obstacles to the deformation after the onset of the plastic flow in the matrix; that is, the deformation of the particles will be entirely accommodated to the flow in the matrix.

Let us suppose a composite of the present type to be subjected to a uniform applied shear stress, τ. Up to the elastic limit, τ is related to the macroscopic shear strain, γ, and the composite shear modulus, μ,

$$\tau = \gamma\mu. \quad (30)$$

It can be considered that the yielding of the composite under consideration occurs when the macroscopic shear strain, γ, reached a yield strain of the matrix. That is, the composite may attain the yielding state when

$$\gamma = \gamma_{ym} = \tau_{ym}/\mu_m, \quad (31)$$

where γ_{ym} is the strain at which the yielding of the matrix without a dispersed phase occurs. Then the overall yield stress can be expressed as

$$\tau_y = \gamma_{ym}\mu = (\mu/\mu_m)\tau_{ym}. \quad (32)$$

Using Equation 5 and expressing in terms of the yield stresses in tension or compression, we obtain

$$\frac{\sigma_y}{\sigma_{ym}} = \frac{\mu}{\mu_m} = 1 + \phi\left[\frac{\mu_m}{\mu_p - \mu_m} + \frac{6(K_m + 2\mu_m)(1-\phi)}{5(3K_m + 4\mu_m)}\right]^{-1}. \quad (33)$$

The indentation hardness of the present composite can now be calculated using Equation 3. If it is assumed that the Poisson's ratios of the two phases are equal and take the values near 0.25, the following relations are obtained

$$E/E_m \simeq \mu/\mu_m = \sigma_y/\sigma_{ym}. \quad (34)$$

Substituting Equation 33 into Equation 3 and taking into account the above relationships, we finally obtain

$$\frac{H}{H_m} = 1 + \phi\left[\frac{\mu_m}{\mu_p - \mu_m} + \frac{6(K_m + 2\mu_m)(1-\phi)}{5(3K_m + 4\mu_m)}\right]^{-1}. \quad (35)$$

Thus, in the present type of composites, the indentation hardness and elastic moduli vary in parallel with volume-fraction of dispersed particles.

For a dilute concentration of dispersed phase, the expression for hardness becomes simpler.

$$\frac{H}{H_m} = \frac{1}{1-\alpha\phi}, \quad (36)$$

where α is given by Equation 9.

3.5. Discussion of theoretical analyses

3.5.1. Hard spherical particles in a soft glass matrix

The overall indentation hardness of the present type of composites can be predicted from Equation 23 for a small concentration of dispersed phase. Equation 23 suggests that the hardness increases with increasing second-phase particles when $Q > 1$ (i.e., $\mu_p > \mu_m$). Indentation testing has shown that, for most homogeneous glasses, typical yield stresses are about $0.03E$ to $0.05E$ (where E is Young's modulus), although they vary from glass to glass [7–9]. In addition, it has been shown that high modulus glasses exhibit generally high indentation hardness [21], which can be related to high yield stresses according to the Marsh theory. A similar argument may be expected to hold for many non-metallic brittle materials [22]. These observations suggest that most composites considered here correspond to the case where $\mu_p > \mu_m$ and hence the hardness is generally increased by the presence of second-phase hard particles.

Equation 23 contains a constant, κ, which depends upon the flow stress and hardness of a glass matrix (Equation 22). From Equation 3, κ can be expressed in terms of E_m and σ_{ym}

$$\kappa = B\,\sigma_{ym}/H_m \quad (22)$$

$$= \left[\frac{A}{B} + \ln\left(\frac{E_m}{3(1-\nu_m)\,\sigma_{ym}}\right)\right]^{-1}. \quad (37)$$

It has been shown that H/σ_y values are typically about 1.5 to 1.7 for most commercial silicate glasses [9, 23]. For organic glasses, values around 1.9 for H/σ_y have been reported [23]. Taking the value for B as 0.60 (determined by Marsh [9]), κ can be then estimated at 0.3 to 0.4 for most glasses. Thus, κ does not change appreciably for a variety of glass matrices. Furthermore, it is important to note that the hardness of a composite has no basic dependence on the particle size and particle spacing. However, the hardness can be indirectly correlated with such microstructural parameters through a stereological expression relating the volume-fraction of dispersed particles to particle size and particle spacing. For randomly distributed particles, the mean free distance between particles, λ, is given by [24].

$$\lambda = \bar{L}_3(1-\phi)/\phi, \quad (38)$$

where $\bar{L}_3$ is the mean intercept length of randomly distributed particles. For a dispersion of spherical particles of diameter, D, $\bar{L}_3$ is given by $2D/3$ [24]. Then, from Equation 38, ϕ can be expressed, for randomly dispersed spheres, as

$$\phi = \frac{D/\lambda}{3/2 + D/\lambda}. \quad (39)$$

Substitution of Equation 39 into Equation 23 or Equation 29 enables the hardness to be expressed in terms of D/λ. Thus, at constant ϕ (i.e., D/λ is constant) the hardness remains constant, even if D and λ vary with one another.

3.5.2. Soft spherical particles in a hard glass matrix

For the present case, the way in which the hardness varies with the volume-fraction of second-phase is determined exclusively by the elastic properties of the two phases. Equation 35 predicts that the hardness will decrease with increasing second-phase particles when $\mu_p < \mu_m$. Contrary to the type of composites discussed in Section 3.5.1, elastic moduli of the matrix must be, for most composites of the present type, higher than those of the dispersed particles. It is therefore expected that the hardness is generally decreased by the presence of second-phase soft particles. Also in this case, the particle size and interparticle spacing do not influence the hardness of the composite if the volume-fraction of the particles is kept constant.

4. Experimental verifications

4.1. Hardness of $PbO-B_2O_3$ immiscible glasses

The Vickers indentation hardness measurements were carried out on lead–borate glasses whose compositions lie in the immiscible region of the $PbO-B_2O_3$ system. Sample preparation technique as well as results of microstructure characterization of the samples studied were already described elsewhere [25, 26]. Specimens about 3 mm thick

TABLE I Hardness data for $PbO-B_2O_3$ immiscible glasses

PbO (wt%)	Volume-fraction of PbO-rich phase	Vickers hardness*	
		H (kgf mm^{-2})	H (GPa)
0	-	123 ± 4	1.21 ± 0.04
5	0.05	131 ± 4	1.28 ± 0.04
10	0.13	146 ± 4.5	1.43 ± 0.04
13	0.18	148 ± 5	1.45 ± 0.05
17	0.25	158 ± 8	1.55 ± 0.08
24		165 ± 4	1.62 ± 0.04
28		161 ± 5	1.58 ± 0.05
32	0.59	240 ± 9	2.35 ± 0.09
36	0.71	281 ± 8.5	2.76 ± 0.08
40	0.84	288 ± 9	2.82 ± 0.09
41	0.88	321 ± 9	3.15 ± 0.09
45	-	370 ± 10	3.63 ± 0.10

*Load, $P = 100$g.

were used for indentation testing. They were finely polished on one surface in kerosene using alumina abrasives to a 0.3 μm finish. Indentation tests were performed on the annealed specimens using a Vickers diamond pyramid with a microhardness tester at room temperature under a dry N_2 environment. At least 20 indentations were made for each specimen with a time of 5 sec at full load of a 100 g weight. The Vickers hardness was calculated from

$$H = 2P\sin(\theta/2)/d^2 , \qquad (40)$$

where d is the average length of diagonals of the indentation, P is the applied load and θ is the angle between opposite faces of the indenter. For the Vickers pyramid, θ is 136°. Table I gives the results of hardness measurements for various glass compositions. The values for the volume-fraction of the PbO-rich phase in Table I were determined by linear analysis of electron micrographs as well as density measurements [25,26].

The immiscible phase boundary for this system has been well characterized. It lies between about 1 to 44 wt% PbO [27]. Microstructural characterization indicates that the glasses under study can be considered as typical particulate composites which are composed of the two end-member phases [25,26,28]. The microstructure consists of PbO-rich spherical particles-B_2O_3-rich matrix for glass compositions on the B_2O_3-rich side of the miscibility gap (about 1 to 20 wt% PbO) and conversely B_2O_3-rich spherical particles–PbO-rich matrix for glass compositions on the PbO-rich side of the gap (about 30 to 44 wt% PbO).

Taking two end-member compositions as 1 wt% PbO and 44 wt% PbO, respectively, the elastic modulus, hardness and flow stress for the end-member phases were estimated. The results are shown in Table II. The value for Young's modulus and Poisson's ratio were obtained by interpolation of the elastic modulus data published by Shaw and Uhlmann [29]. The values for hardness were estimated by interpolation of the experimental data listed in Table I. Flow stresses were calculated from hardness and Young's modulus values following the theory of Marsh [9].

For glass compositions on the B_2O_3-rich side within the miscibility gap, the dispersed second-phase has higher elastic modulus and higher flow stress. In addition, the glasses in this composition

TABLE II Elastic modulus, hardness and flow stress data estimated for the end-member phases which form $PbO-B_2O_3$ immiscible glasses

End-member phase	Young's modulus*, E(GPa)	Poisson's ratio*, ν	Hardness, H(GPa)	Flow stress,† σ_y (GPa)
1 wt% PbO glass	17.5	0.26	1.23	0.716
44 wt% PbO glass	56.5	0.27	3.53	1.92

*After Shaw and Uhlmann [29].
†Evaluated from the theory of Marsh [9].

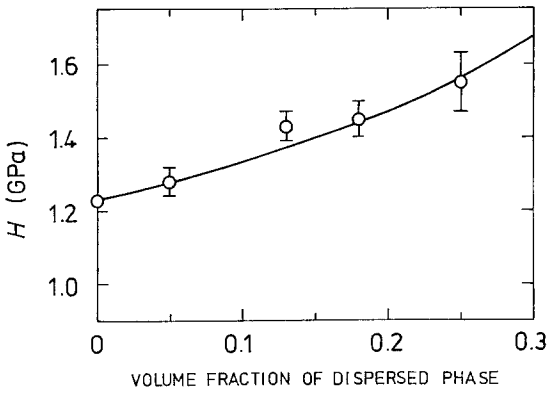

Figure 1 Variation of Vickers hardness with volume-fraction of dispersed phase for glasses consisting of PbO-rich particles–B_2O_3-rich matrix. The solid curve represents Equation 23.

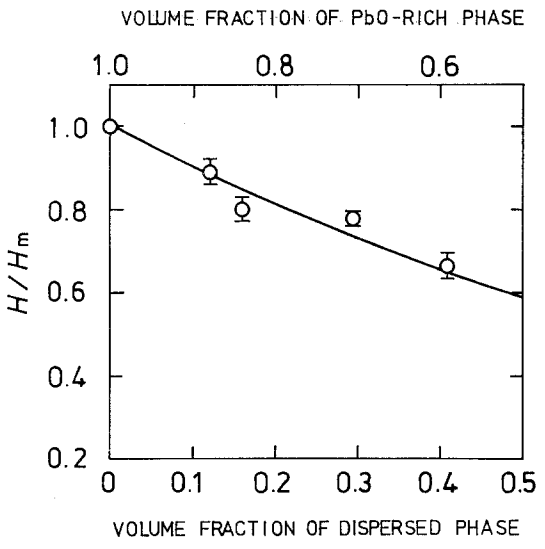

Figure 2 Reduced Vickers hardness for glasses consisting of B_2O_3-rich particles–PbO-rich matrix plotted against the volume-fraction of dispersed phase. Solid curve represents Equation 35.

range present relatively small volume-fractions of dispersed phase. It is then expected that the hardness behaviour follows Equation 23 derived for a composite consisting of hard particles–soft glass matrix. In Fig. 1, the indentation hardness observed for glass on the B_2O_3-rich side of the miscibility gap is plotted against the volume-fraction of dispersed PbO-rich phase. The solid curve in the figure represents theoretical prediction established from Equation 23. It is seen from Fig. 1 that the experimental data are in fair agreement with the theory.

For glass compositions on the PbO-rich side within the miscibility gap, it is expected that the presence of the second-phase dispersion causes a reduction of the hardness and its behaviour is explained following Equation 35. In Fig. 2, the experimental hardness data for the glasses under consideration are plotted against the volume-fraction of dispersed B_2O_3-rich phase. The theoretical prediction established from Equation 35 is illustrated by a solid curve. It is found that the experimental hardness varies with volume-fraction of dispersed second-phase in accordance with the theoretical prediction.

4.2. Hardness of a phase-separated sodium borosilicate glass

Another set of Vickers indentation experiments was carried out on a Vycor-type sodium borosilicate glass having the composition 60 mol% SiO_2 30 mol% B_2O_3 10 mol% Na_2O. It has been shown that this type of glass consists of two principal phases, one rich in silica which seems to be perfectly homogeneous and the other rich in borate containing a microphase of sodium borate [30]. For the glass composition selected for study, the microphase rich in silica remains discontinuous and forms discrete spherical particles. Prod'homme [31] and Cordelier [32] followed, using replication electron microscopy, the development of phase-separation morphology of the present glass as a function of applied heat-treatment temperature and time.

The glass* was subjected to an isothermal heat-treatment for increasing times at 710° C, corresponding to the optimal opacification temperature for this glass. Microstructural analysis was carried out on each heat-treated sample using replication electron micrographs taken by Cordelier [32]. The glass specimens about 3 mm thick were used for Vickers indentation testing. Hardness measurements were carried out using a Vickers diamond pyramid with a hardness tester in air at room temperature. At least 10 indentations were made on each specimen surface with a time of 10 sec at full load of a 100 g weight. Table III summarizes the results of microstructure characterization and hardness measurements for glass specimens subjected to various heat-treatment times at 710° C.

*The glass was supplied by the Société Sovirel to the Laboratoire des Verres du CNRS, Paris, directed by Dr A. Winter. One of the authors (NM) carried out some experimental work on this glass during his stay in the laboratory.

TABLE III Vickers hardness for a phase-separated sodium borosilicate glass subjected to an isothermal heat-treatment at 710° C for various times

Heat treatment time at 710° C (h)	Volume-fraction of silica-rich phase	Particle diameter* D (nm)	Vickers hardness†	
			H (kgf mm^{-2})	H (GPa)
(As cooled)	-	-	486 ± 17	4.77 ± 0.17
1	0.12	100	487 ± 18	4.78 ± 0.18
2	0.17	130	505 ± 25	4.95 ± 0.25
4	0.21	180	487 ± 19	4.78 ± 0.19
8	0.26	220	478 ± 14	4.69 ± 0.14
16	0.31	260	476 ± 24	4.67 ± 0.24
32	0.28	330	480 ± 17	4.71 ± 0.17
64	0.29	420	475 ± 23	4.66 ± 0.23
128	0.31	540	476 ± 20	4.67 ± 0.20

*After Cordelier [32].
†Load, $P = 100$ g.

An attempt has been made to interpret hardness data for this glass regarding it as a two-phase particulate composite, consisting of silica-rich spherical particles in a borate-rich matrix. However, the data must be interpreted semi-quantitatively due to a lack of detailed knowledge concerning constituent properties of the present phase-separated glass. It can be assumed that this glass corresponds to a composite containing a second-phase dispersion with a higher elastic limit. As silicate glasses containing a large amount of B_2O_3 and Na_2O generally present lower elastic moduli than glasses highly rich in silica [33], the elastic modulus for the continuous matrix is presumed to be lower than that for the silica-rich dispersed phase. It is then expected that the hardness behaviour can be explained on the basis of the theoretical analysis given in Section 3.3.

In Fig. 3, the Vickers hardness, volume-fraction of dispersed silica-rich particles and particle size are plotted against the heat-treatment time at 710° C. It is seen that the average particle size varies clearly in proportion to the cube root of heat-treatment time after 6 h of treatment. Further the volume-fraction of dispersed silica-rich phase is found to reach a constant value, 0.30 after 8 h of heat-treatment. These observations suggest that after about 8 h of heat-treatment, the composition of the matrix remains unaltered and the micro-structural modification results entirely from the coarsening mechanism of particles. As indicated from Equation 38 or 39, the ratio of the inter-particle spacing to the particle size is constant when the volume-fraction of dispersed phase remains unaltered. Therefore, when the coarsening mechanism proceeds the inter-particle spacing should also vary in proportion to the particle size. It is found that the hardness remains constant after 8 h of heat-treatment. This hardness behaviour is in accord with the theoretical prediction (Equation 23). Thus, the hardness is independent of the particle size and inter-particle spacing as long as the volume-fraction of dispersed phase is constant.

For the initial stage of heat-treatment at

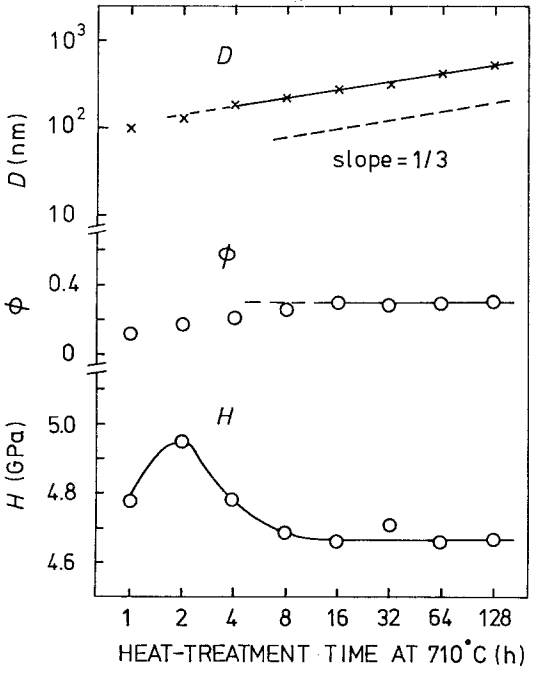

Figure 3 Variation of dispersed particle size, D, volume-fraction of dispersed particles, ϕ, and Vickers hardness, H, for a sodium borosilicate glass as a function of heat-treatment time at 710° C. The particle size data is after Cordelier [32].

710° C (up to about 6 h), the situation is rather complicated. A slight increase in volume-fraction of dispersed particles with heat-treatment time at this stage leads us to imagine that the coarsening may not be a sole phenomenon which occurs in the phase-separation process. It seems that the ionic diffusion process still occurs to some extent. In fact, dielectric measurements carried out on the same glass samples suggest a possible variation of the chemical composition of the matrix at this heat-treatment stage [34]. It can be assumed, therefore, that the hardness and elastic modulus of the matrix decrease with increasing heat-treatment time due to the decrease in silica content of the matrix chemcial composition. On one hand, the increase in volume-fraction of the hard, silica-rich phase may contribute to increasing the hardness of the composite. On the other hand, the variation of the matrix composition may contribute to decreasing it. The hardness variation at the initial stage of heat-treatment may be then explained as follows: up to about 2 h of heat-treatment, the hardness decrease of the matrix resulting from the variation of the chemical composition is presumed to be small and the overall hardness increases with increasing heat-treatment time owing to the increase in volume-fraction of silica-rich phase; however, after about 2 h, the hardness of the matrix may decrease appreciably with heat-treatment time and the overall hardness decreases despite the small increases in volume-fraction of silica-rich phase.

5. Application of the theory to a glass-ceramic

Tashiro and Sakka [35,36] measured the Vickers hardness of a partially crystallized Li_2O–SiO_2 glass-ceramic, derived from the glass of composition 81 wt % SiO_2 12.5 wt % Li_2O 2.5 wt % K_2O 4 wt % Al_2O_3 0.03 wt % CeO and 0.027 wt % Au. The base glass specimens were irradiated for various times by ultra-violet light. After the u.v. exposure, each specimen was subjected to heat-treatment at 510° C for 30 min and successively at 620° C for 60 min. The crystal phase was identified as lithium metasilicate crystal ($Li_2O \cdot SiO_2$) by X-ray diffraction. It was found, by X-ray analysis and density measurements, that the proportion of the crystal phase was constant after heat-treatment at 620° C for 60 min, regardless of the difference in u.v. exposure time. In Table IV, the Vickers hardness data are shown along with the crystallite size determined from electron micrographs. This glass-ceramic contains a large proportion of glass phase (about 55 wt %) and hence is regarded as glass matrix composite with a hard particle dispersion. The constancy of the proportion of the crystal phase suggests that the composition of the glass matrix remains unaltered for all of the specimens subjected to the u.v. exposure. Although the crystal shape is not spherical and the concentration of crystal phase is relatively large, the general hardness behaviour can be appreciated on the basis of our theory. The Vickers hardness is found to be independent of the particle size in accordance with the theoretical analysis which predicts that the hardness of composite remains unchanged as long as the volume-fraction of second-phase is constant.

TABLE IV Vickers hardness of a partially crystallized Li_2O–SiO_2 glass-ceramic*

U.v. exposure time (min)	Crystallite size (nm)	Vickers hardness, H (kgf mm^{-2})
0	0	560
2	620	830
30	340	828
180	290	845
600	462	830
1000	525	830

*Data from Tashiro and Sakka [35, 36].

6. Concluding remarks

The present analysis on the indentation hardness of glass matrix, particulate composite is based upon the assumption that glass is an elastic–plastic solid on a microscopic scale. Although this assumption is rather phenomenological, the theoretical analyses were in good agreement with the experimental results of the Vickers hardness for phase-separated PbO–B_2O_3 and Na_2O–B_2O_3–SiO_2 glasses. The theory could also give a good explanation of published data for the Vickers hardness of a glass-ceramic. However, it should be noted that there are some glasses whose deformation process is believed to be dominated by the densification mechanism. In this respect, further study should be undertaken to analyse the hardness of glass matrix composites for possible cases where inelastic deformation in the matrix is dominated by densification and to examine the degree to which the overall hardness behaviour of the composite reflects the deformation mechanism in the matrix.

Acknowledgements

The authors are indebted to Mr T. Nishida for experimental assistance. The hardness measurement for Na_2O–B_2O_3–SiO_2 glass was carried out in the Laboratoire des Verres, CNRS, Institut d'Optique, Paris. One of the authors (NM) is grateful to Dr L. Prod'homme for his helpful suggestions and encouragement.

References

1. I. W. DONALD and R. A. McCURRIE, *J. Amer. Ceram. Soc.* **55** (1972) 289.
2. A. J. STRYJAK and P. W. McMILLAN, *J. Mater. Sci.* **13** (1978) 1275.
3. *Idem, ibid.* **13** (1978) 1794,
4. R. W. RICE, *ibid* **14** (1979) 2678.
5. M. N. TURETZKY, J. B. JENKINS and H. R. FRASER, Jr., *J. Electrochem. Soc.* **121** (1974) 1098.
6. R. W. DOUGLAS, *J. Soc. Glass Techn.* **42** (1958) 145.
7. E. W. TAYLOR, *ibid* **34** (1950) 69.
8. L. AINSWORTH, *ibid* **38** (1954) 479, 501.
9. D. M. MARSH, *Proc. Roy. Soc. (London)* **A279** (1964) 420.
10. F. M. ERNSBERGER, *J. Amer. Ceram. Soc.* **51** (1968) 545.
11. J. E. NEELY and J. D. MACKENZIE, *J. Mater. Sci.* **3** (1968) 603.
12. K. W. PETER, *J. Non-Cryst. Solids* **5** (1970) 103.
13. D. TABOR, "The Hardness of Metals" (Clarendon Press, Oxford, 1951).
14. R. HILL, "The Mathematical Theory of Plasticity" (Clarendon Press, Oxford, 1950) p. 97.
15. S. M. WIEDERHORN, *J. Amer. Ceram. Soc.* **52** (1969) 99.
16. E. H. KERNER, *Proc. Phys. Soc. (London)* **B69** (1956) 808.
17. Z. HASHIN, *J. Appl. Mech.* **29** (1962) 143.
18. J. D. ESHELBY, *Proc. Roy. Soc. (London)* **A241** (1957) 376.
19. K. TANAKA and T. MORI, *Acta Met.* **18** (1970) 931.
20. G. E. DIETER, "Mechanical Metallurgy", Second edition (McGraw-Hill Book Co., New York, 1976).
21. J. D. MACKENZIE, "Mechanical Behaviour of Materials", Vol 4 (The Society of Materials Science, Japan, 1972) p. 347.
22. A. KELLY, "Strong Solids", Second edition (Clarendon Press, Oxford, 1973) Table 3 in Appendix A.
23. G. M. BARTENEV, I. V. RAZUMOVSKAYA and D. S. SANDITOV, *J. Non-Cryst. Solids* **1** (1969) 388.
24. E. E. UNDERWOOD, "Quantitative Stereology" (Addison-Wesley, Reading, Massachusetts, 1970) p. 80.
25. N. MIYATA and H. JINNO, *J. Non–Cryst. Solids* **38/39** (1980) 391.
26. *Idem, J. Mater. Sci.* **16** (1981) 2205.
27. J. ZARZYCKI and F. NAUDIN, *Phys. Chem. Glasses* **8** (1967) 11.
28. R. R. SHAW and D. R. UHLMANN, *J. Non-Cryst. Solids* **1** (1969) 474.
29. *Idem, ibid* **5** (1971) 237.
30. W. VOGEL, "Structur und Kristallisation der Gläser" (VEB Deutscher Verlag für Grundstoffindustrie, Leipzig, 1965).
31. L. PROD'HOMME, in "Influence des Changements de Phase sur les Propriétés Physiques des Corps Solides", edited by J. P. Suchet (Masson, Paris, 1970) p. 155.
32. J. F. CORDELIER, *Verres Réfract.* **24** (1970) 113.
33. H. SCHOLZE, "Glas–Natur, Structur und Eigenschaften", French edition, translated by J. Le Dû (Institut du Verre, Paris, 1974).
34. N. MIYATA, *Verres Réfract.* **33** (1979) 13.
35. M. TASHIRO and S. SAKKA, *J. Ceram. Assoc. Japan* **68** (1960) 158.
36. M. TASHIRO, *Glass Ind.* **47** (1966) 428.

Received 6 May
and accepted 15 July 1981